Since January 2020 Elsevier has created a COVID-19 resource centre with free information in English and Mandarin on the novel coronavirus COVID-19. The COVID-19 resource centre is hosted on Elsevier Connect, the company's public news and information website.

Applied Mathematical Modelling 90 (2021) 466–473

Contents lists available at ScienceDirect

Applied Mathematical Modelling

journal homepage: www.elsevier.com/locate/apm

Analytical features of the SIR model and their applications to COVID-19

Nikolay A. Kudryashov[a], Mikhail A. Chmykhov[a], Michael Vigdorowitsch[b,*]

[a] Department of Applied Mathematics, National Research Nuclear University MEPhI (Moscow Engineering Physics Institute), 31 Kashirskoe Shosse, Moscow 115409, Russian Federation
[b] Angara GmbH, In der Steele 2, Düsseldorf 40599, Germany

ARTICLE INFO

Article history:
Received 20 June 2020
Revised 2 August 2020
Accepted 14 August 2020
Available online 28 September 2020

Keywords:
SIR-model
Nonlinear differential equation
First integral
Infection
Solution
Coronavirus

ABSTRACT

A classic two-parameter epidemiological SIR-model of the coronavirus propagation is considered. The first integrals of the system of non-linear equations are obtained. The Painlevé test shows that the system of equations is not integrable in the general case. However, the general solution is obtained in quadrature as an inverse time-function. Using the first integrals of the system of equations, analytical dependencies for the number of infected patients $I(t)$ and that of recovered patients $R(t)$ on the number of susceptible to infection $S(t)$ are obtained. A particular attention is paid to interrelation of $I(t)$ and $R(t)$ both depending on α/β, where α is the contact rate in the community and β is the intensity of recovery/decease of patients. It is demonstrated that the data on particular morbidity waves in Hubei (China), Italy, Austria, South Korea, Moscow (Russia) as well some Australian territories are satisfactorily described by the expressions obtained for $I(R)$. The variability of parameter N having been traditionally considered as a static population size is discussed.

1. Introduction

The SARS-Cov-2 pandemic has introduced an evident research boom into biophysical and mathematical modeling of infection expansions. Main efforts have been related to identification of factors [1–12] that help prognosticate the pandemic development what is a clear concern in the atmosphere of anxiety and social limitations. Among a variety of infection expansion model types, the SIR- (susceptible-infectives-recovered, where infectives are indistinguishable from ill) models occupy a particular place. On the one hand, they physiologically better correspond to the SARS-Cov-2 case with immunity for recovered unlike the simplest SIS- (susceptible-infectives-susceptible) model type [13], and on the other hand, they provide as a two-parametric tool an ultimately transparent modeling compared to advanced and sophisticated multi-factor models [14].

Although the SIR-model history is going to celebrate its centenary jubilee [15], its purely analytical solutions have appeared just lately. One of them is represented by a time series expansion that has a need for an approximate analytical continuation since the series are characterised by a limited convergence radius and therefore inapplicable in the case of long durations [16]. Another one [14] has a parametric form of inverse functions in quadrature, featured through its inte-

* Corresponding author.
E-mail address: mv016@yahoo.com (M. Vigdorowitsch).

https://doi.org/10.1016/j.apm.2020.08.057
0307-904X/

gration limits with a functionally modified time-dependent variable which complicates both analysis and application. The model does not seem to have ever undergone the Painlevé test.

The SIR-model in its classic formulation has the following form: the numbers $S(t)$ of those who are susceptible, $I(t)$ for infectives and $R(t)$ for recovered (and deceased that belong to the same category group within the model), who freely contact one another with the disease transmission factor contact rate α and recover (and decease) with factor β within an isolated homogeneous community, are interrelated through the following set of equations:

$$S_t = -\alpha\, I S, \tag{1}$$

$$I_t = \alpha\, I S - \beta\, I, \tag{2}$$

$$R_t = \beta\, I \tag{3}$$

Despite a number of attempts having been undertaken to study the properties of set (1)–(3), interdependencies between time functions $S(t)$, $I(t)$ and $R(t)$ still remain to a certain extent uncovered. Obtaining such compartmental relations would give rise to applications of the SIR-model to discrete processes. Besides that, the search potential for a better analytical time-dependent solution has not yet been exhausted. The purpose of this paper is to deeply consider analytical properties of the classic SIR-model and to assess its applicability to the SARS-Cov-2 case.

2. The Painlevé test and the first integrals of the SIR model

First of all, it is attractive to test the SIR-model for the Painlevé property to estimate related analytical solution perspectives. Through differentiation over t, Eqs. (1) and (2) appear to be reducible to the second-order nonlinear differential equation:

$$I\, I_{tt} - I_t^2 + \alpha\, I^2\, I_t + \alpha\, \beta\, I^3 = 0. \tag{4}$$

A one-parameter analytical solution of Eq. (4) exists in the form

$$I(t) = \tilde{C}_1\, \exp(-\beta\, t), \tag{5}$$

where $\tilde{C}_1$ is an arbitrary constant.

To understand the integrability of the SIR model we apply the Painlevé test to Eq. (4), following to the Kovalevskaya algorithm [17–21]. Using the first step of the Painlevé test, we have

$$I = \frac{1}{\alpha\, (t - t_0)} + \dots, \tag{6}$$

where t_0 is arbitrary constant. As the second step, we find Fuchs indices corresponding to expansion of solution $I(t)$ in Laurent series, to be $j_{1,2} = \pm 1$. However, upon substituting the Laurent series for solution $I(t)$ in the form

$$I = \frac{1}{\alpha\, (t - t_0)} + I_1 + I_2\, (t - t_0) + \dots, \tag{7}$$

we find out that I_1 cannot be arbitrary, and there are no meromorphic solutions of Eq. (4) for $\beta \neq 0$. With $\beta = 0$, Eq. (4) is transformable to the well-known Riccati equation

$$I_t + \alpha\, I^2 - \tilde{C}_2\, I = 0, \tag{8}$$

where $\tilde{C}_2$ is the constant of integration. Eq. (8) is well-known to pass the Painlevé test and to represent an integrable equation of the first order. Thus, Eq. (4) is not integrable in the general case.

Nevertheless, there are two first integrals for the SIR model. Equality

$$R_t + I_t + S_t = 0 \tag{9}$$

is an obvious consequence of set (1)–(3) and gives rise to the first integral

$$S(t) + I(t) + R(t) = N, \tag{10}$$

where N appears to be integration constant typically [15] set to the community's population. Eq. (10) enables us to transform Eq. (2) into

$$I_t = \alpha\, I(N - R - I) - \beta\, I. \tag{11}$$

Should Eq. (4) be once integrated, Eq. (11) could serve for determination of the integration constant since it helps transform Eq. (3) into Eq. (4). Another first integral has the form

$$\beta + \frac{I_t}{I} - \beta\, \ln\left\{\beta + \frac{I_t}{I}\right\} + \alpha\, I = C_1 \tag{12}$$

which can be checked through direct substitution into Eq. (4). Most naturally, C_1 may be determined while linked to the extremal value of function I_p at $t = t_p$ provided epidemiological data with a peak were available:

$$C_1 = \beta - \beta \ln\{\beta\} + \alpha I_p. \tag{13}$$

That there is just one extremal point is a direct consequence of Eq. (12) and to be easily proved through the assumption for a while that there are multiple extremal points. Further comments to determination of this integration constant follow beneath.

3. Solution of the SIR model

Introducing function $Y = \frac{I_t}{I}$ we make a transition from the first integral (12) to the relation

$$Y(I) = \left\{\exp\left[\frac{\alpha I - C_1}{\beta} - \frac{1}{\beta} W\left(-\frac{1}{\beta} \mathrm{e}^{\frac{\alpha I - C_1}{\beta}}\right)\right] - \beta\right\}, \tag{14}$$

where $W(x)$ is Lambert function [22], which gives rise to the solution of the SIR-model in quadrature with the still undetermined integration constant C_1:

$$t = t_0 + \int \frac{I\,dI}{\left\{\exp\left[\frac{\alpha I - C_1}{\beta} - \frac{1}{\beta} W\left(-\frac{1}{\beta} \mathrm{e}^{\frac{\alpha I - C_1}{\beta}}\right)\right] - \beta\right\}}. \tag{15}$$

The Lambert function $W(x)$ introduces a quaintness into solution (15) as it has an essentially negative argument giving rise to real-valued range space with $x \in [-\frac{1}{e}; 0)$ only. $W(x)$ is a double-valued function thereby reasonably referring to the values of t before and after the peak of $I(t)$. At the peak, both branches of $W(x)$ meet one another at $x = -\frac{1}{e}$.

Since $W(x)$ possesses complicated asymptotics, solution (15) is not easy to deal with. What can be said in general is that $I(t)$ is a bell-shaped function with a unique maximum. Therefore, we should use the chance to learn more about the properties of the SIR-model through its first integrals (10) and (12). Eqs. (10) and (11) enable us to retrieve the following equations:

$$\beta + \frac{I_t}{I} = \alpha(N - R - I) = \alpha S. \tag{16}$$

which, while combined with the first integral (5), leads to

$$I(S) = \frac{\beta}{\alpha} \ln\{\alpha S\} - S + \frac{C_1}{\alpha}. \tag{17}$$

Through division of Eq. (3) by Eq. (1), we obtain

$$\frac{dR}{dS} = -\frac{\beta}{\alpha S}. \tag{18}$$

and further

$$R(S) = C_2 - \frac{\beta}{\alpha} \ln\{S\}. \tag{19}$$

Similarly, one can obtain Eq. (17) while dividing Eq. (2) by Eq. (1).

The integration constants are to be found from the initial conditions:

$$I(t = 0) = M, \qquad S(t = 0) = N - M, \qquad R(t = 0) = 0 \tag{20}$$

so that C_1 and C_2 read

$$C_1 = \alpha N - \beta \ln\{\alpha N - \alpha M\}, \qquad C_2 = \frac{\beta}{\alpha} \ln\{N - M\}, \tag{21}$$

and we can explicitly link both I and R with S:

$$I(S) = N - S + \frac{\beta}{\alpha} \ln\left(\frac{S}{N - M}\right) \tag{22}$$

and

$$R(S) = \frac{\beta}{\alpha} \ln\left(\frac{N - M}{S}\right). \tag{23}$$

One can note that we have from Eqs. (22) and (23) the formula

$$I = N - R - (N - M) \exp\left\{-\frac{\alpha R}{\beta}\right\}. \tag{24}$$

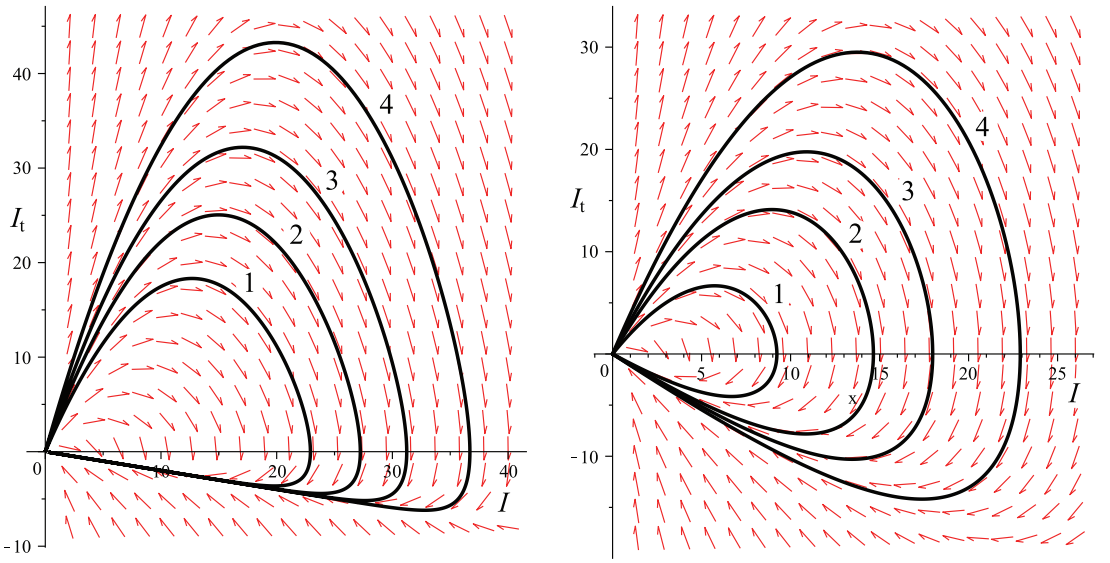

Fig. 1. Phase plane portrait of Eq. (4) for $\alpha = 0.1$, $\beta = 0.2$, $I_t(t = 0) = 5.0$, $I(t = 0) = 1.9$ (curve 1), $I(t = 0) = 1.6$ (curve 2), $I(t = 0) = 1.4$ (curve 3), $I(t = 0) = 1.2$ (curve 4)(on the left) and for $\alpha = 0.1$, $\beta = 1.2$, $I_t(t = 0) = 2.0$, $I(t = 0) = 1.1$ (curve 1), $I(t = 0) = 0.7$ (curve 2), $I(t = 0) = 0.6$ (curve 3), $I(t = 0) = 0.5$ (curve 4)(on the right).

Eqs. (22) –(24) can be used for fruitful analysis of epi-/pandemic expansion. Indeed, the maximum number of infectives that follows from Eq. (22) is reached at $S_p = \frac{\beta}{\alpha}$ and equal to

$$I_p = N + \frac{\beta}{\alpha}\left[\ln\left(\frac{\beta}{\alpha N - \alpha M}\right) - 1\right]. \tag{25}$$

Thus, this peak value corresponds to the unique $t = t_p$, unlike all the other magnitudes of $I(t)$ due to the bell-shaped form of functions $I(t)$ and $I(S)$. Therefore, as it follows from the double-valuedness of Lambert function and can be easily checked, the peak value of $I(t)$ corresponds to that argument of Lambert function in Eq. (15) where its branches meet one another.

With C_1 and C_2 in Eq. (21), we can write solution (15) in its final form as

$$t = t_0 + \int \frac{I\, dI}{\exp\left[\frac{\alpha(I-N)-\beta\ln\{\alpha(N-M)\}}{\beta} - \frac{1}{\beta} W\left(-\frac{1}{\beta} e^{\frac{\alpha(I-N)-\beta\ln\{\alpha(N-M)\}}{\beta}}\right)\right] - \beta}. \tag{26}$$

Now we undertake some analysis and discussion of the two-parameter SIR model solution.

4. Results and discussion

The second-order Eq. (4) for the number of infected individuals has a single stationary point on the phase plane $(I, I_t) = (0, 0)$ what makes its phase portrait look quite simple. In Fig. 1 we present some phase plane portrait for this equation at $\alpha = 0.1$, $\beta = 0.2$ (in the left hand side) and $\alpha = 0.1$, $\beta = 1.2$ (in the right hand side). From Fig. 1 it follows that the phase trajectories depend on parameters α and β as well as being significantly sensitive to initial conditions for the function $I(t)$ and its derivative.

Interpretation of data on infected, recovered and susceptible appears to be convenient in terms of their interrelations rather than as time-dependencies. Characteristic shapes of functions $I(S)$ and $R(S)$ are illustrated in Fig. 2. Note that increase in susceptibles is always oppositely directed to the time arrow for any SIR-model, if $N = const$.

An important feature of the SIR model, that seems to have been underevaluated so far is that to model the development of an epi-/pandemic, one does not necessarily have to do this in terms of time-dependent functions. Thus, employment of dependance $I(R)$ for these purposes appears to be quite fruitful as it follows from Fig. 3. We can see, how sensitive to initial data is the SIR model. This circumstance is illustrated in Fig. 3, where the results of calculating the dependencies $I(R)$ are presented at various N and β.

Furthermore, the results obtained make us re-visit the essence of parameter N. Typically associated with the community's population, N does not seem to belong to given data for communities and, moreover, does not have to be necessarily constant which, in particular, has been noted in [23] earlier. Fig. 3 demonstrates how the changes in N, α and β lead to significant quantitative changes in the number of infected and recovered individuals. The reasons matter why α and β can vary. Contact factor α is sure to depend on social structure and population behavioural model. Indeed, it represents index

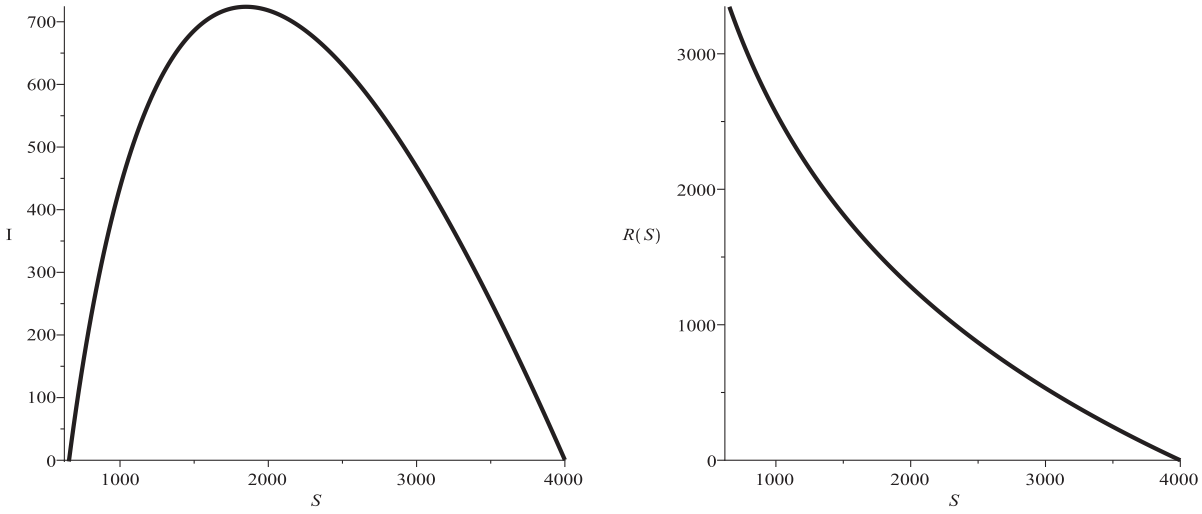

Fig. 2. Dependencies I(S) (on the left) and R(S) (on the right) for $N = 3699$, $M = 1$, $\alpha = 0.00001$, $\beta = 0.0165$.

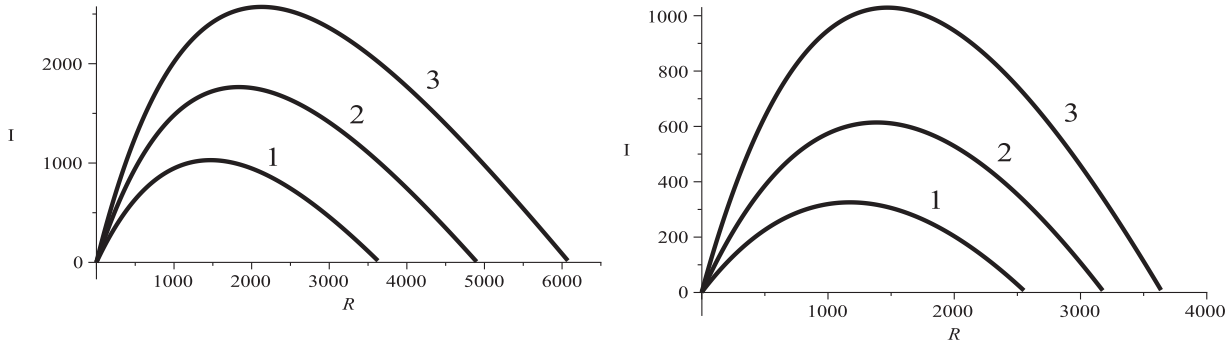

Fig. 3. Dependencies $I(R)$ at various values N at $\alpha = 0.00001$, $\beta = 0.015$, $N_1 = 4000$ (curve 1), $N_2 = 5100$ (curve 2) and $N_3 = 6200$ (curve 3)(on the left) and at $\alpha = 0.00001$, $N = 4000$, $\beta_1 = 0.015$ (curve 1), $\beta_2 = 0,002$ (curve 2), $\beta_3 = 0.0025$ (curve 3) (on the right).

$\alpha =< \alpha >$ averaged out over different groups. Identification of these groups represents a separate task. For example, individuals older than 60 years may potentially be characterised as more susceptible than younger individuals, what can potentially result in $\alpha_{> 60}$ or $\alpha_{< 60}$, because, while infected, older people are to have more probably to restrict their behavioural activities to a greater extent consequently reducing the related subgroup contact rate.

Eqs. (24) and (25) are to be used in the following manner. We calculate first the ratio α/β at the peak value (25) for infected. To do this, we are to employ some value of N that, generally speaking, remains undefined. We define it as the accumulated number of infected to be known at the moment $N = N_p + I_p + R_p$. The corresponding dependence $I(R)$ is presented in Figs. 4–6 in green.

Furthermore, we use alternative definitions of N as well, among whose are $N = N_{max}$ (total number of infected during the whole epi-/pandemic) and a bit greater $N = 1.1\,N_{max}$. These new definitions of N have been introduced to calculate new ratios α/β to be used to calculate the corresponding dependencies $I(R)$. Calculated values α/β are presented in the table, and the corresponding curves are coloured red and blue.

Country / Region	N_p	$\frac{\alpha}{\beta}$	N_{max}	$\frac{\alpha}{\beta}$	$1.1 \cdot N_{max}$	$\frac{\alpha}{\beta}$
China, Hubei	61,682	3.74e04	68135	2.08e04	74949	1.37e04
Italy	178,972	4.30e05	228658	2.16e05	251520	1.72e05
Russia, Moscow	149,607	1.16e04	175829	5.51e05	193412	3.94e05
Diamond Princess	705	0.49	712	0.30	783	0.05
Northern Territory, Australia	27	6.01	29	1.59	32	0.68
Australia	5687	5.64e03	7099	1.54e03	7809	1.07e03

The dependencies $I(R)$ for Hubei (China) and Italy, for Moscow (Russia) and cruise ship Diamond Princess, for Australian'n northern territory and whole Australia are presented in Figs. 4–6, respectively. The data origin for relevant communities is [24,25]. From these figures we see that the two-parameter SIR model, when applied to countries and big cities, gives a

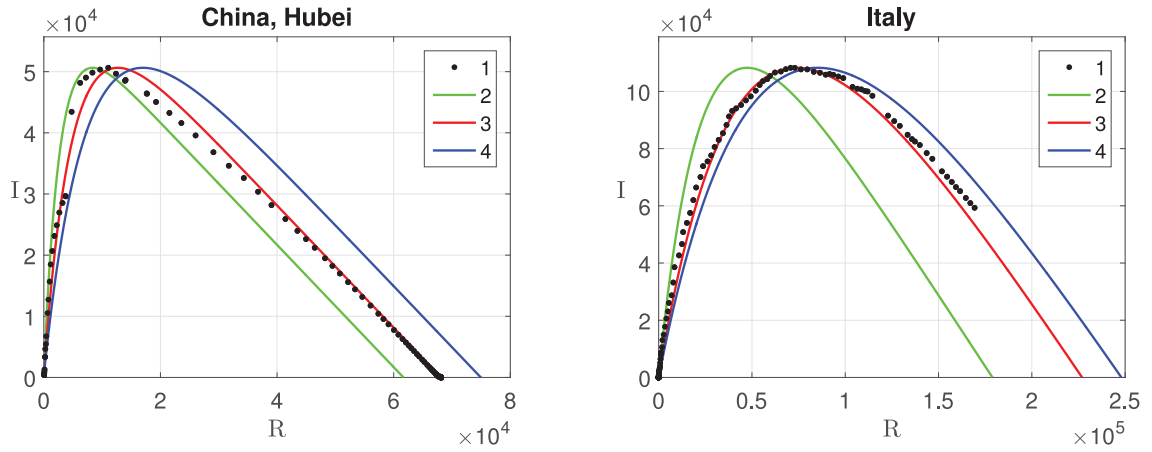

Fig. 4. Dependencies $I(R)$ due to formula (24) with the data for Hubei (China) (on the left) and Italy (on the right). 1: data from the database [24], date intervals from 22-Jan-2020 to 22-May-2020; 2: due to formula (24) for $N = N_p$; 3 — (24) for $N = N_{max}$; 4 — (24) for $N = 1.1 \cdot N_{max}$. (For interpretation of the references to color in this figure legend, the reader is referred to the web version of this article.)

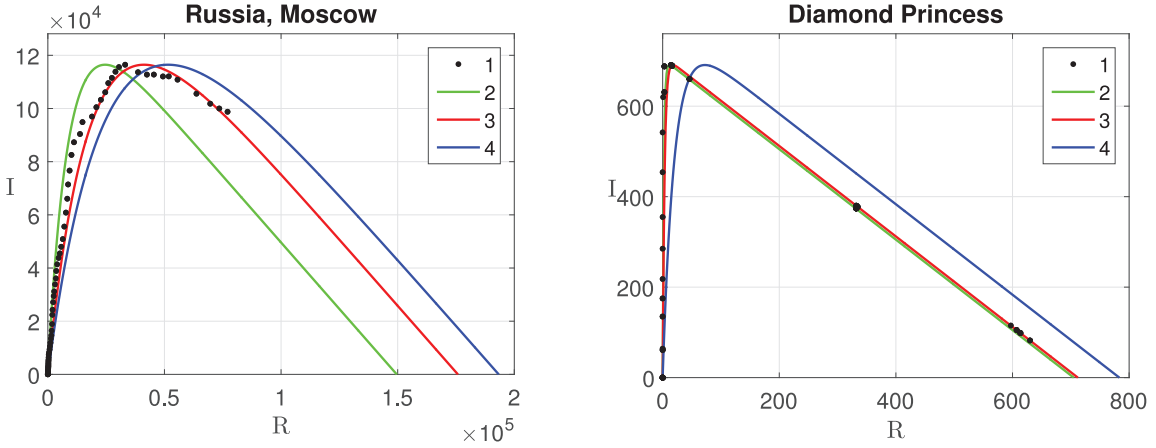

Fig. 5. Dependencies $I(R)$ due to by formula (24) with the data for population of Moscow (Russia) (in the left hand side, date intervals from 15-Mar-2020 to 29- May-2020) and for cruise ship Diamond Princess (in the right hand side, date intervals from 22-Jan-2020 to 22-May-2020). 1: data from the database [24,25]; 2: due to (24) for $N = N_p$; 3: (24) for $N = N_{max}$; 4: (24) for $N = 1.1 \cdot N_{max}$. (For interpretation of the references to color in this figure legend, the reader is referred to the web version of this article.)

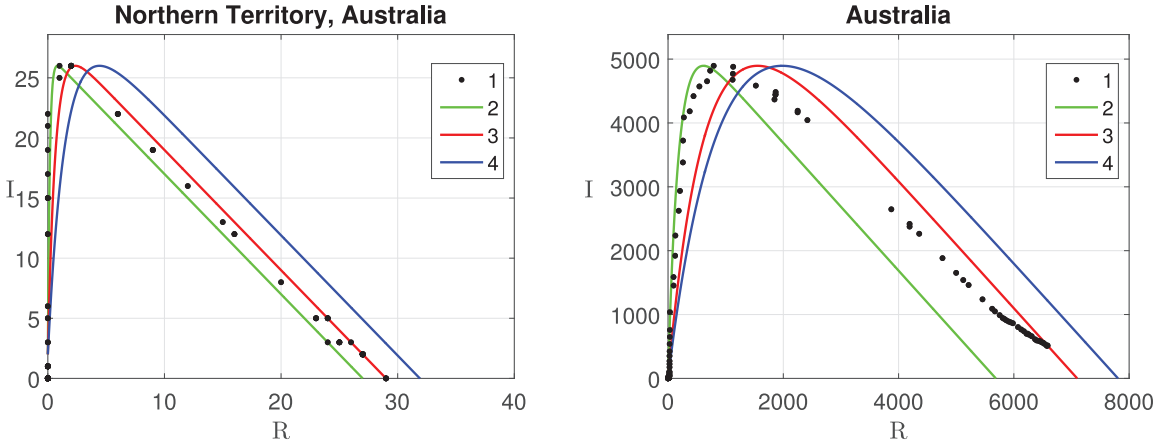

Fig. 6. Dependencies $I(R)$ due to formula (24) with data for northern territory of Australia (on the left) and for Australia as a whole (on the right). 1: data from the database [24], date intervals from 22-Jan-2020 to 22-May-2020; 2: due to Eq. (24) for $N = N_p$; 3: (24) with $N = N_{max}$; 4: (24) with $N = 1.1 \cdot N_{max}$. (For interpretation of the references to color in this figure legend, the reader is referred to the web version of this article.)

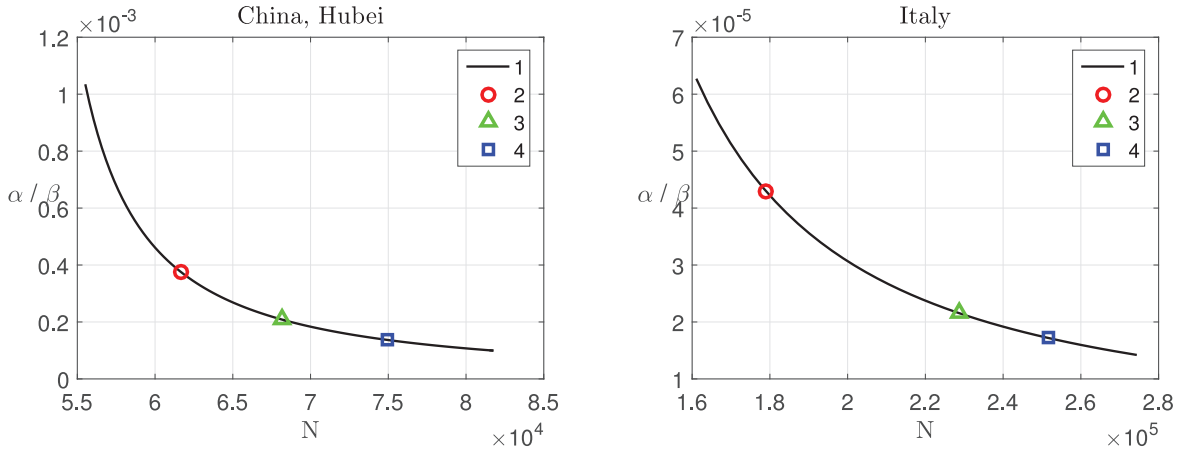

Fig. 7. Dependencies $\frac{\alpha}{\beta}(N)$ for Hubei (China) (on the left) and Italy (on the right). 1: numerical results; 2: $N = N_p$; 3: $N = N_{max}$; 4: $N = 1.1 \cdot N_{max}$.

rather satisfactory match with the data on infected and recovered individuals at certain values of variable indicators such as contact rate α and characteristics N of the community.

We found out that parameters N and α/β, while considered as phenomenological in the two-parameter SIR model, are dependent on one another. As Ns change, so do the values of α/β. These dependencies are shown for Hubei (China) and for Italy in the Fig. 7. The green, red and blue markers in Fig. 7 correspond to the curves shown in Fig. 1.

5. Conclusion

In this paper, we have considered a classic two-parameter epidemiological SIR-model and applied this to the case SARS-Cov-2. The model parameters, α and β, represent the contact and recover/decease rates respectively. Besides those, the results are being affected through the initial conditions to which belongs N traditionally considered as the population size.

A analytical treatment enabled us to obtain the first integrals of the system of non-linear equations, one of them does not appear to have been known before. Despite the Painlevé test does not indicate integrability in the general case, we have obtained a general solution of the model in quadrature as an inverse time-function. Although the analytical form of the solution is not perfect, it is free of some of disadvantages inherent to the analytical solutions having been obtained before. A part of the general solution, function $I(t)$ for infectives, is expected to be linked to an epidemiological peak, providing the broadest domain for the general solution. We have analyzed dependencies of infectives and recovered on susceptible and found out that within the classic two-parametric SIR-model the best fit with realistic epidemiological data takes place when parameter N is considered close to the accumulated amount of infectives, starting from the pan-/epidemic beginning. This is to be interpreted rather as a feature of the classic two-parametric SIR model than as an effective reduction of those who are susceptible to infection because of self-isolation of the rest. With such an interpretation of N, the data for particular morbidity waves in Hubei (China), Italy, Germany, Russia and cruise liner Diamond Princess considered as sample cases are satisfactorily described by fitting dependencies $I(R)$.

Generally speaking, the results obtained mean that the applicability of the SIR-model is restricted because of indefiniteness of parameter N that appears to depend, in fact, on communities behavioural characteristics. The latter can produce the epi-/pandemic second and further waves whose description in the framework of the SIR-model can follow through adjustment of the initial conditions. Furthermore, indefiniteness of N makes it reasonable to perform trial calculations for various values of the parameter.

The SIR-model is limited to relatively small populations for which it is capable of producing good results. This is a useful tool even when the $I(R)$ curve cannot be so well fitted because it might suggest how the basic SIR model needs to be modified. To the model advantages belong its parametrical simplicity as well as transparency in the sense of its solution expressed in terms of compartmental relations on the basis of the first integral uncovered in this study. Indeed, these relations represent the invariants and enable one to avoid time-dependences what gives rise to description of irregular or even discontinuous processes. The final equations for compartments are simple and can serve for estimates to be performed by everyone.

Declaration of Competing Interest

The authors also declare that there is no conflict of interest.

Acknowledgments

This research was supported by Russian Foundation for Basic Research (N. A. K. and M. A. C.) according to the research project No. 18-29-10025.

References

[1] D. Fanelli, F. Piazza, Analysis and forecast of COVID-19 spreading in China, Italy and France, Chaos Solitons Fractals 134 (2020) 109761.
[2] Z. Chladni, J. Kopfov, D. Rachinskii, S.C. Rouf, Global dynamics of SIR model with switched transmission rate, J. Math. Biol. 80 (2020) 1209–1233, doi:10.1007/s00285-019-01460-2.
[3] B. Tang, N.L. Bragazzi, Q. Li, S. Tang, Y. Xiao, J. Wu, An updated estimation of the risk of transmission of the novel Coronavirus (2019-ncov), Infect. Dis. Model. 5 (2020) 248–255.
[4] T. Sun, Y. Wang, Modeling COVID-19 epidemic in Heilongjiang province, China, Chaos Solitons Fractals 138 (2020) 109949.
[5] H. Swapnarekha, H.S. Behera, J. Nayak, B. Naik, Role of intelligent computing in COVID-19 prognosis: a state-of-the-artreviewchaos, Solitons Fractals 138 (2020) 109947.
[6] O. Torrealba-Rodriguez, R.A. Conde-Gutiérrez, A.L. Hernández-Javier, Modeling and prediction of COVID-19 in Mexico applying mathematical and computational models, Chaos Solitons Fractals 138 (2020) 109946.
[7] M.J. Willisa, V.H.G. Diaz, O.A. Prado-Rubio, M. von Stosch, Insights into the dynamics and control of COVID-19 infection rates, Chaos Solitons Fractals 138 (2020) 109937.
[8] B. Zhou, X. Zhang, D. Jiang, Dynamics and density function analysis of a stochastic SVI epidemic model with half saturated incidence rate, Chaos Solitons Fractals 138 (2020) 109865.
[9] R. Salgotra, M. Gandomi, A.H. Gandomi, Time series analysis and forecast of the COVID-19 pandemicin india using genetic programming, Chaos Solitons Fractals 138 (2020) 109945.
[10] B.K. Mishraa, A. K. Keshri, Y.S. Rao, B.K. Mishra, B. Mahato, S. Ayesha, B.P. Rukhaiyyar, D.K. Saini, A.K. Singh, COVID-19 created chaos across the globe:three novel quarantine epidemic models, Chaos Solitons Fractals 138 (2020) 109928.
[11] P. Melin, J.C. Monica, D. Sanchez, O. Castillo, Analysis of spatial spread relationships of coronavirus(COVID-19) pandemic in the world using self organizing maps, Chaos Solitons Fractals 138 (2020) 10917.
[12] S. Lalwan, G. Sahni, B. Mewarab, R. Kumar, Predicting optimal lockdown period with parametric approach using three-phase maturation SIRD model for COVID-19 pandemic, Chaos Solitons Fractals 138 (2020) 109939.
[13] H.W. Hethcote, The mathematics of infectious diseases, SIAM Rev. 42 (2000) 599–653.
[14] N.S. Barlow, S.J. Weinstein, Accurate closed-form solution of the SIR epidemic model, Physica D 408 (2020) 132540. htttp://www.doi.org/10.1016/j.physd.2020.132540.
[15] W.O. Kermack, A.G. McKendrick, A contribution to the mathematical theory of epidemics, Proc. R. Soc. Lond. Ser. A 115 (1927) 700–721.
[16] T. Harko, F.S.N. Lobo, M.K. Mak, Exact analytical solutions of the susceptible-infected-recovered (SIR) epidemic model and of the SIR model with equal death and birth rates, Appl. Math. Comput. 236 (2014) 184–194, doi:10.1016/j.amc.2014.03.030.
[17] M.J. Ablowitz, H. Segur, Exact linearization of a Painleve transcendent, Phys. Rev. Lett. 38 (1977) 1103–1106.
[18] M.J. Ablowitz, H. Segur, A connection between nonlinear evolution equations and ordinary differential equations of P-type. I, J. Math. Phys. 21 (1980) 715–721.
[19] N.A. Kudryashov, Painlevé analysis and exact solutions of the Korteweg-de Vries equation with a sourse, Appl. Math. Lett. 41 (2015) 41–45.
[20] N.A. Kudryashov, Painlev e analysis and exact solutions of the fourth-order equation for description of nonlinear waves, Commun. Nonlinear Sci. Numer. Simul. 28 (1–3) (2015) 1–9.
[21] N.A. Kudryashov, Simplest equation method to look for exact solutions of nonlinear differential equations, 2005. 24, 5, 1217–1231.
[22] R.M. Corless, G.H. Gonnet, D.E.G. Hare, D.J. Jefrey, D.E. Knuth, On the lambert w function. advances in computational mathematics, 1996, 5, 329–359.
[23] A.C. Osemwinyen, A. Diakhaby, Mathematical modelling of the transmission dynamics of Ebola virus, Appl. Comput. Math. 4 (2015) 313–320.
[24] E. Dong, H. Du, L. Gardner, a) COVID-19 data repository by the center for systems science and engineering (CSSE) at Johns Hopkins University, An interactive web-based dashboard to track COVID-19 in real time. Lancet Inf Dis, 20, 2020, pp. 533–534. [Online]. Available: https://github.com/CSSEGISandData/COVID-19, folder COVID-19/csse-covid-19-data/csse-covid-19-time-series/. [Accessed: 22-May-2020]; b). doi:10.1016/S1473-3099(20)30120-1.
[25] CORONAVIRUS today monitoring the spread of COVID-19 in the world, 2020. [Online]. Available: https://xn—-7sbgffetn1ahcahtfqb7a0v.xn–p1ai/. [Accessed: 29-May-2020] (in Russian).